COMMUNICATION

ChemComm
www.rsc.org/chemcomm

Cruciform π-systems: hybrid phenylene-ethynylene/phenylene-vinylene oligomers†

James N. Wilson, Mira Josowicz, Yiqing Wang and Uwe H. F. Bunz*

Department of Chemistry and Biochemistry, Georgia Institute of Technology, 770 State St., Atlanta, GA, 30332, USA. E-mail: uwe.bunz@chemistry.gatech.edu; Fax: 01 404 385 1795; Tel: 01 404 385 1795

Received (in Columbia, MO, USA) 30th September 2003, Accepted 22nd October 2003
First published as an Advance Article on the web 11th November 2003

The cruciform pentamers 3a–g were synthesized by a combined Horner–Sonogashira approach; their band gaps vary significantly with emission varying from blue to red depending upon their substituent pattern.

Conjugated materials are important as active layers in device applications. Poly(*para*phenylenevinylene)s (PPV) have proved to be tremendously successful in device fabrication, due to their balanced hole and electron injection capabilities.[1] Recently, polymers that combine the structural features of poly(*para*phenyleneethynylene)s (PPE), and those of PPVs have been reported.[2] Formal hybrids such as **A** behave considerably more like PPEs[3] than like PPVs. However, if styryl groups are laterally attached to the benzene rings the electronic properties of the resulting polymer **B** are different from both PPV and PPEs.[4] Is the change in properties indigenous to the polymer backbone, or are single, isolated, cruciforms "cut out" of **B** responsible for the observed electronic effects? We find that the optical, electronic and redox properties of **B** reside mostly in their pentameric cruciform[5] modules **3**.

Starting from the bisphosphonate **1** a Horner[6] reaction produced the distyrylbenzenes **2a–e** in good to excellent yields (Scheme 1). In the second step **2a–e** were coupled to terminal alkynes utilizing $(Ph_3P)_2PdCl_2$ and CuI in piperidine.[7] In the case of the synthesis of **3g** triethylamine was utilized to avoid nucleophilic addition of piperidine to the aromatic nucleus. In the cases of **3c,d** the products were quite insoluble and therefore the yield was lower than average (53% and 63%); **3a–g** were purified by double crystallization.

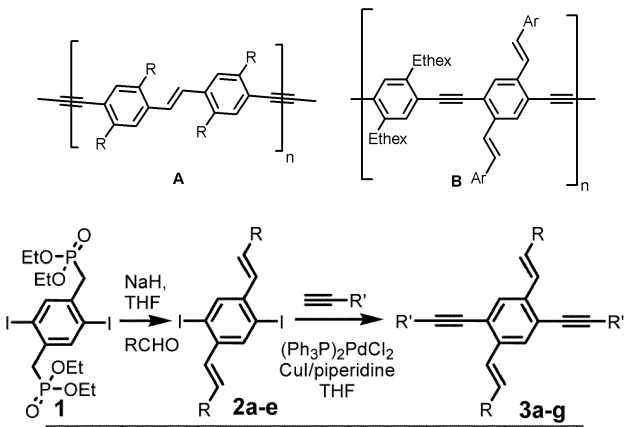

	3a	3b	3c	3d	3e	3f	3g
R							
R'							
2	79%	77%	61%	72%	72%	-	-
3	81%	77%	53%	63%	91%	67%	76%

Scheme 1 Two-step reaction scheme, substituent key and yields of compounds **2a–e** and **3a–g**.

The absorption data of **3a–g** are shown in Figs. 1 and 2 and in Table 1. The λ_{max} values correspond qualitatively with the expected ordering predicted from the substituent patterns. Cruciform **3d** has the largest and **3g** the lowest optical band gap. The three oligomers **3e–g** show a nice correlation of decreasing band gap with increasing CF_3 substitution. The donor–acceptor interaction decreases the band gap. To obtain more information we investigated the electrochemistry of **3a–g**. The cruciforms **3a–g** show oxidation potentials that are in qualitative agreement with their calculated (RHF 6-31G**, Fig. 1) HOMO values. The electrochemical reduction data is difficult to interpret for **3e–g** due to electron-transfer induced reactions that lead to dull,

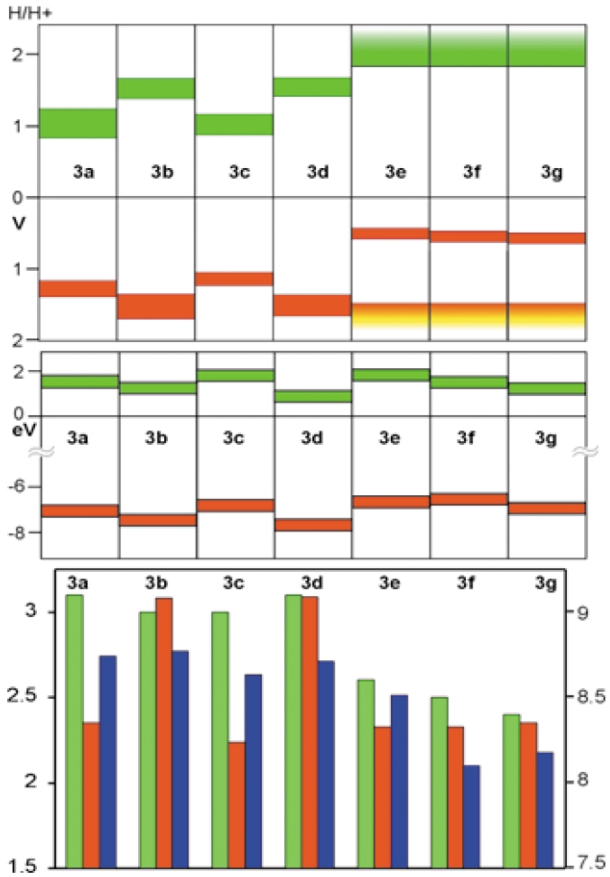

Fig. 1 Top: electrochemical bandgap with reduction in green and oxidation in red (**3a–g**). Faded regions correspond to an onset of oxidation/reduction that does not reach a peak value. The range of each bar corresponds to the onset and peak values. Middle: calculated bandgaps (reduction: green, oxidation: red). Bottom: comparison of optical (green, eV), electrochemical (red, V), and calculated (blue, scale at right, eV) bandgaps.

† Electronic supplementary information (ESI) available: details of the synthesis of **3**. See http://www.rsc.org/suppdata/cc/b3/b312156a/

DOI: 10.1039/b312156a

Table 1 Summary of the absorbance and emission data of cruciforms **3** in chloroform and hexane; **3d** is insoluble in hexane. **3a–d** show similar spectra in both hexane and chloroform, while **3e–g** show dramatic solvatochromicity in emission

	3a	**3b**	**3c**	**3d**	**3e**	**3f**	**3g**
Ab. $CHCl_3$	331, 365 sh	330	339,374 sh	330, 363 sh	339, 439	342, 444	345, 458
Em. $CHCl_3$	420, 442	446, 526 sh	432, 454	419, 434 sh	514	543	563
Φ $CHCl_3$[a]	0.83	0.28	0.88	0.92	0.16	0.20	0.14
Ab. hex	326, 352 sh	324, 348 sh	334, 376 sh	—	332, 422	344, 416	346, 420
Em. hex	414, 432	424, 444 sh	420, 442	—	472, 498	502, 526 sh	524
Φ hex[a]	0.78	0.45	0.78	—	0.94	0.70	0.53

[a] Vary by ±5%.

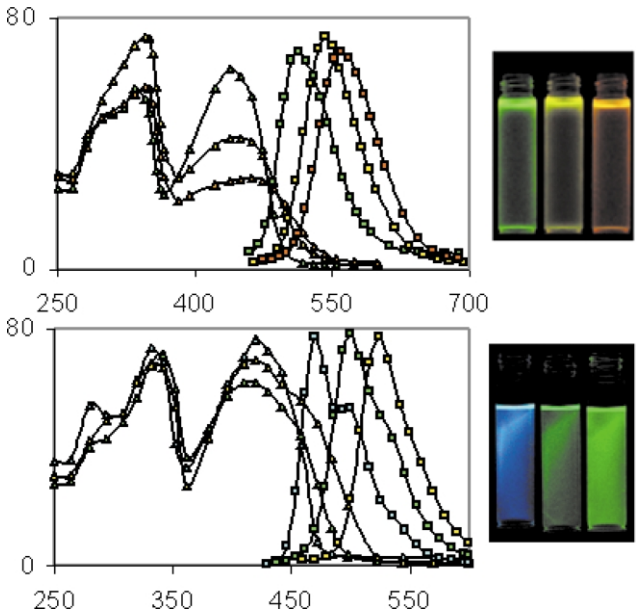

Fig. 2 The series of dibutylamino compounds (top) in chloroform: **3e** (grn), **3f** (yel), **3g** (org). Absorbance (triangles) shows varying peak height, but the same position, while emission (squares) clearly shows a 20+ nm shift on inclusion of CF_3 substituents. These compounds also show high solvatochromicity: the emissions of the compounds in chloroform are substantially red-shifted from their emissions in hexane (bottom), **3e** (blu), **3f** (grn), **3g** (yel).

colored deposits on the electrodes. Thus, only onset values are given for **3e–g**. The reduction of **3c** is easier than expected in comparison to the calculated value, while the reduction potential of **3d** is higher than expected. Not surprisingly, **3d** is the most difficult, and **3e** is most easily oxidized while the electron-rich cruciforms **3e–g** show a second irreversible oxidation wave.

In solution all of the cruciforms were highly fluorescent ($0.45 < \Phi < 0.94$) in hexane. In chloroform the emission quantum yields were lower for **3b** and **3e–g**. The cruciforms **3a–d** are blue emitters but **3e–g** show dramatic differences in their emission that are also solvent dependent. In chloroform (Fig. 2 top) the emission of **3e–g** changes from green to orange, while in hexane a similar trend is observed, however, the color changes from blue–green to yellow (Fig. 2 bottom, Table 1). In methanol the emission of **3g** is weak and red. Similar effects are observed for **3e** and **3f**.

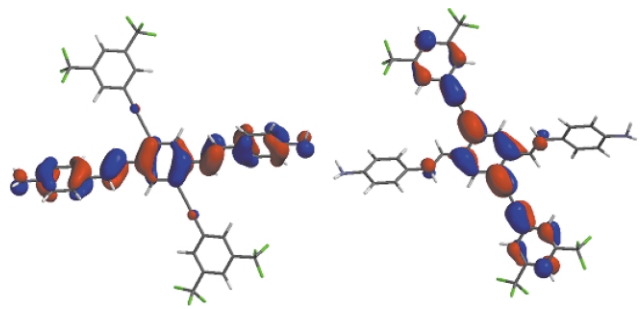

Fig. 3 RHF 6-31G** calculated structure of **3g** (butyl groups omitted). Left: HOMO of **3g**. Right: LUMO of **3g**. The HOMO is almost completely localized on the distyrylbenzene branch of the cruciform, while the LUMO is almost fully localized on the aryleneethynylene substructure.

The frontier orbitals of **3g** were inspected (RHF 6-31G**, Spartan). The HOMO is localized on the distyrylbenzene branch of the cruciform while the LUMO is localized on the phenyleneethynylene part (Fig. 3). HO and LU orbitals overlap only in the central benzene ring. The insensitivity of the oxidation potential of **3e–g** upon introduction of CF_3 groups into the molecule is a consequence of the spatial separation of the HOMO and the LUMO. For **3a** this type of de-mixing of the HOMO and LUMO is not observed and both orbitals are almost evenly distributed over the whole molecule. The excited states of **3e–g** must show charge separation, which explains the sensitivity of their emission wavelength towards the polarity of the solvent. An increasingly polar solvent stabilizes the excited state and leads to a bathochromically shifted emission.

In summary we have made cruciforms **3** and examined their electronic properties. They are model compounds for polymers of the type **B**. Conjugation along the backbone does not seem to have a significant effect on **B**. The cruciforms **3** are versatile and tuneable chromophores where the position of the HOMO and LUMO can be changed almost at will by the introduction of electron donating and electron accepting substituents. The localization of the HOMO on the PV branch and that of the LUMO at the PE branch makes **3** cross-conjugated in a non-classical sense and extends this attractive concept.[8,9]

The authors thank the National Science Foundation (CHE 0138-659, PI Bunz) for funding. UHFB is a Camille Dreyfus Teacher-Scholar (2000-2004).

Notes and references

1 A. Kraft, A. C. Grimsdale and A. B. Holmes, *Angew. Chem., Int. Ed.*, 1998, **37**, 402.
2 G. Brizius, N. G. Pschirer, W. Steffen, K. Stitzer and H.-C. zur Loye, *J. Am. Chem. Soc.*, 2000, **122**, 12435; D. A. M. Egbe, H. Tillmann, E. Birckner and E. Klemm, *Macromol. Chem. Phys.*, 2001, **202**, 2712.
3 C. E. Halkyard, M. E. Rampey, L. Kloppenburg, S. L. Studer Martinez and U. H. F. Bunz, *Macromolecules*, 1998, **31**, 8655.
4 J. N. Wilson, P. M. Windscheif, U. Evans, M. L. Myrick and U. H. F. Bunz, *Macromolecules*, 2002, **35**, 8681.
5 J. E. Klare, G. S. Tulevski, K. Sugo, A. de Picciotto, K. A. White and C. Nuckolls, *J. Am. Chem. Soc.*, 2003, **125**, 6030.
6 L. Horner, H. Hoffmann and H. G. Wippel, *Chem. Ber.*, 1958, **91**, 61; L. Horner and W. Klink, *Tetrahedron Lett.*, 1964, **36**, 2467.
7 K. Sonogashira, *J. Organomet. Chem.*, 2002, **653**, 46; E. Neghishi and L. Anastasia, *Chem. Rev.*, 2003, **103**, 1979; U. H. F. Bunz, *Chem. Rev.*, 2000, **100**, 1605.
8 Y. M. Zhao and R. R. Tykwinski, *J. Am. Chem. Soc.*, 1999, **121**, 458; R. R. Tykwinski, M. Schreiber, V. Gramlich, P. Seiler and F. Diederich, *Adv. Mater.*, 1996, **8**, 226.
9 H. Hopf, *Classics in Hydrocarbon Chemistry*, Wiley-VCH, Weinheim, 2000.